Corridors of barchan dunes: Stability and size selection

P. Hersen,[1] K. H. Andersen,[2] H. Elbelrhiti,[3] B. Andreotti,[1] P. Claudin,[4] and S. Douady[1]

[1]*Laboratoire de Physique Statistique de l'ENS, 24 rue Lhomond, 75005 Paris, France*
[2]*Department of Mechanical Engineering, Technical University of Denmark, DK-2800 Lyngby, Denmark*
[3]*Faculté des Sciences, Université Ibn Zohr, BP 28/S, Cité Dakhla, 80000 Agadir, Morocco*
[4]*Laboratoire des Milieux Désordonnés et Hétérogènes (UMR 7603), 4 place Jussieu-case 86, 75252 Paris Cedex 05, France*

Barchans are crescentic dunes propagating on a solid ground. They form dune fields in the shape of elongated corridors in which the size and spacing between dunes are rather well selected. We show that even very realistic models for solitary dunes do *not* reproduce these corridors. Instead, two instabilities take place. First, barchans receive a sand flux at their back proportional to their width while the sand escapes only from their horns. Large dunes proportionally capture more sand than they lose, while the situation is reversed for small ones: therefore, solitary dunes cannot remain in a steady state. Second, the propagation speed of dunes decreases with the size of the dune: this leads, through the collision process, to a coarsening of barchan fields. We show that these phenomena are not specific to the model, but result from general and robust mechanisms. The length scales needed for these instabilities to develop are derived and discussed. They turn out to be much smaller than the dune field length. As a conclusion, there should exist further, yet unknown, mechanisms regulating and selecting the size of dunes.

PACS number(s): 45.70.Qj, 45.70.Vn, 89.20.−a

Since the pioneering work of Bagnold [1], sand dunes have become an object of research for physicists. Basically, the morphogenesis and the dynamics of dunes result from the interaction between the wind, which transports sand grains and thus modifies the shape of the dune, and the dune topography which in turn controls the air flow. A lot of works have been devoted to the study of the mechanisms at the scale of the grain [2–17] and at the scale of a single dune [18–41]. The interested reader should refer to a previous paper [42] for a review of these works. Our aim is to focus here on dune fields and to show that most of the problems at this scale are still open or even ill-posed.

The most documented type of dune, the barchan [46], is a crescentic shaped dune, horns downwind, propagating on a solid ground. In the general picture emerging from the literature, barchans are thought as solitary waves propagating downwind without changing their shape and weakly coupled to their neighborhood. For instance, most of the field observations concern geometric properties (morphologic relationships) and kinematic properties (propagation velocity). This essentially static description probably results from the fact that barchans do not change a lot at the timescale of one field mission.

As shown on Fig. 1, barchans usually do not live isolated but belong to rather large fields [43]. Even though they do not form a regular pattern, it is obvious that the average spacing is a few times their size, and that they form long *corridors* of quite uniformly sized dunes. Observing the right part of Fig. 1, the barchans have almost all the same size (6 m to 12 m high, 60 m to 120 m long and wide). Observing now the left part of Fig. 1, the barchans are all much smaller (1.5 m to 3 m high, 15 m to 30 m long and wide) and a small band can be distinguished, in which the density of dunes becomes very small. Globally, five corridors stretched in the direction of the dominant wind can be distinguished: from right to left, no dune, large dunes, small dunes, no dune and small dunes again. Figure 1 shows only 17 km of the barchan

field but direct observations show that these five corridors persist in a *coherent* manner over the 50 km along the dominant wind direction without any natural obstacle. The field itself remains composed of dunes between 1 m and 12 m along its 300 km.

The content of this paper is perhaps a bit unusual as we will mostly present *negative* results. Indeed, we will show
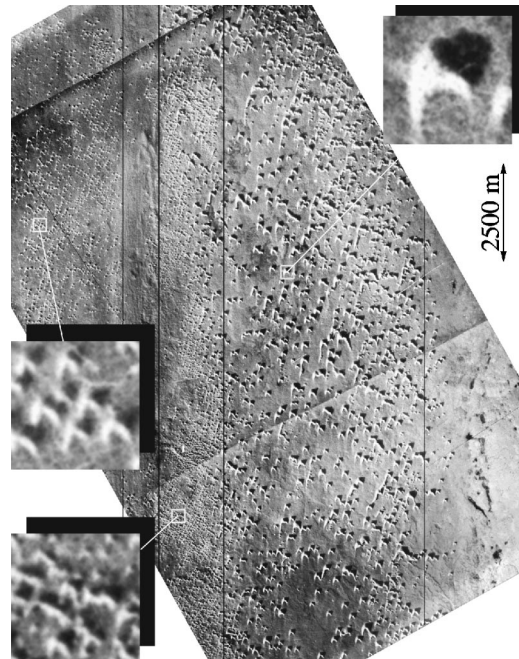

FIG. 1. Aerial photograph showing part of the barchan field extending between Tarfaya, Laayoune and Sidi Aghfinir in southern Morocco, former Spanish Sahara. The trade winds, dominant in the region, blow from the north (from the top of the photograph). Several corridors are visible in which the size of barchans and their density is almost uniform. As confirmed by the three zooms, the size of dunes is different from one corridor to another.

that none of the dune models [33–41], nor the coarse grained field simulation [44] are able at present to reproduce satisfactorily the selection of size and the formation of these corridors.

More precisely, we shall first address the stability of solitary dunes, and conclude that, given reasonable orders of magnitude for dune sizes and velocities, barchans which are considered as ''marginally unstable'' by other authors [41] would in fact have the time to develop their instability over a length much smaller than that of the corridor they belong to. As a consequence, isolated dunes must be considered as truly unstable objects. Furthermore, the origin of this instability is rather general and model independent, as it can be understood from the analysis of the output sand flux as a function of the dune size.

One can wonder whether interactions via collisions between dunes can modify the dynamics and the stability of dunes. In a recent paper Lima *et al.* [44] have investigated the dynamics of a field and have claimed to get realistic barchan corridors. However, they made use of numerical simulations into which individual dunes are stable objects of almost equal size (6% of polydispersity). They consequently obtained a nearly homogeneous field composed of dunes whose width is that of those injected at the upwind boundary. We show here that the actual case of individually unstable dunes leads by contrast to an efficient coarsening of the barchan field.

The paper is organized as follows. In order to get a good idea of the mechanisms leading to these two instabilities, we first derive a 3D generalization of the C_C^C model previously used to study 2D dunes [28]. We then show that the two instabilities predicted by the C_C^C model are in fact very general and we will derive in a more general framework the time and length scales over which they develop. Turning to field observations, we will conclude that the formation of nearly uniform barchan corridors is an open problem: there should exist further mechanisms, not presently known and may be related to more complicated and unsteady effects such as storms or change of wind direction, to regulate the dune size.

I. BARCHAN MODELING. THE C_C^C MODEL

We start here with the state of the art concerning the modeling of dunes by Saint-Venant like equations. First, the mechanisms of transport at the scale of the grain [2,4–17,42] determine at the macroscopic scale—at the scale of the dune—the maximum quantity of sand that a wind of a given strength can transport. As a matter of fact, when the wind blows over a flat sand bed, the sand flux increases and saturates to its maximum value Q after a typical length L called the saturation length [1,16,28,29]. This length determines the size of the smallest propagative dune.

The other part of the problem is to compute the turbulent flow around a huge sand pile of arbitrary shape [30,31]. Since the Navier-Stokes equations are far too complicated to be completely solved, people have derived simplified descriptions of the turbulent boundary layer [32–41]. The first step initiated by Jackson and Hunt has been to derive an explicit expression of the basal shear stress in the limit of a very flat hill. Kroy *et al.* [40,41] have shown that this expression can be simplified without loosing any important physical effect. In particular, it keeps the nonlocal feature of the velocity field: the wind speed at a given place depends on the whole shape of the dune.

Being a linear expansion, this approach can not account for boundary layer separation and in particular for the recirculation bubble that occurs behind dunes. Following Zeman and Jensen [31] and later Kroy *et al.*, the Jackson and Hunt formula is in fact applied to an envelope of the dune constituted by the dune profile prolonged by the separation surface.

As already stated in one of our previous papers [28], we proposed to name C_C^C the class of models which describe the dynamics of dunes in terms of the dune profile h and the sand flux q, and which include (i) the mass conservation, (ii) the progressive saturation of sand transport and (iii) the feedback of the topography on the sand erosion/deposition processes. We chose this fancy name in reference to the spatial organization of the dunes which propagate like the flight of wild ducks and geese.

A. 2D and 3D main equations

Let us start with a quick recall of the set of 2D C_C^C equations that we already introduced in [28]. Let x denote the axis oriented along the wind direction, and t the time. The continuity equation which ensures mass conservation simply reads

$$\partial_t h + \partial_x q = 0. \tag{1}$$

Note that $q(x,t)$ denotes the integrated *volumic* sand flux, i.e., the volume of sand that crosses at time t the position x per unit time. The saturation process is modeled by the following charge equation

$$\partial_x q = \frac{q_{sat} - q}{L}. \tag{2}$$

It is enough to incorporate the fact that the sand flux follows the saturated flux q_{sat} with a spatial lag L. It is a linearized version of the charge equation proposed by Sauermann *et al.* [16].

The saturated flux q_{sat} is a growing function of the shear stress. This shear stress can be related to the dune profile h by the modified Jackson and Hunt expression. Since this expression comes from a linear expansion, we can directly relate q_{sat} to h by

$$\frac{q_{sat}(x)}{Q} = 1 + A \int \frac{d\chi}{\pi \chi} \partial_x h_e(x-\chi) + B \partial_x h_e(x), \tag{3}$$

where Q is the saturated flux on a flat bed and h_e the envelope prolonging the dune on the lee side (see Appendix and [28,40] for the details of construction). The last term takes into account slope effects, while the convolution term encodes global curvature ones. The only relevant length scale is the saturation length L of the sand flux. The other relevant physical parameter is the saturated sand flux on a flat bed Q.

All the lengths are calculated in units of L, time in units of Q/L^2, and fluxes in unit of Q. A and B could in principle be predicted by the Jackson and Hunt analysis but we rather take them as two tunable phenomenological constants.

In three dimensions, equations are very similar, albeit slightly different. In order to express the total sand flux (which is now a 2D vector), we need to distinguish saltons and reptons [45]. The reason is that in contrast to the saltons, which *follow the wind*, the motion of the reptons is sensitive to the local slope [3]. Because the reptons are dislodged by the saltons, we assume that their fluxes are proportional [17], so that the total flux can be written as the sum of two terms, one along the wind direction $\vec{x}$ and the other along the steepest slope [3]:

$$\vec{q}_{\text{tot}} = q\vec{x} - Dq\vec{\nabla}h. \tag{4}$$

The continuity equation then takes its generalized form

$$\partial_t h + \vec{\nabla} \cdot \vec{q}_{\text{tot}} = 0. \tag{5}$$

The down slope flux of reptons acts as a diffusive process. The diffusion coefficient is proportional to q so that no new scale is introduced—D is a dimensionless parameter. This diffusion term introduces a nonlinearity that has a slight effect only: almost the same dynamics is obtained if a constant diffusion coefficient is used instead. Equations (2) and (3) can be solved independently in each slice along x.

In summary, the C_C^C model considered here includes in a simple way all the known dynamical mechanisms for interactions between the dune shape, the wind and the sand transport.

B. Propagative solutions of the C_C^C model

In a previous paper [28], we have studied in details steady propagative solutions in the 2D case. They also apply to transverse dunes, i.e., invariant in the y direction. We will now focus on three dimensional solitary dunes computed with the C_C^C model presented in the latter section. The details of the integration algorithm and the numerical choice of the different parameters can be found in the Appendix and a more detailed discussion about the influence of the diffusion parameter is discussed in [45]. Figure 2 shows in stereoscopic views the time evolution of an initial conical sand pile ($t=0$). Horns quickly develop ($t=16$ and $t=32$) and a steady barchan shape is reached after typically $t=50$. Note that the propagation of the dune is not shown on Fig. 2: the center of mass of the dune is always kept at the center of the computation box.

The original C_C^C model proposed by Kroy, Sauermann, and Hermann [40,41] was the first of a long series of models in which a steady solitary solution could be exhibited, with all the few known properties of barchans. In particular, the dunes present a nice crescentic shape with a length, a width, a height and a horn size that are related to each others by linear relationships. They propagate downwind with a velocity inversely proportional to their size, as observed on the field. These properties are robust inside the class of modeling, since we get the same results with the simplified version

that we use here. We will only show in the following two of these properties, important for the stability discussion, namely the velocity and the volume as functions of the dune size.

Since they are linearly related one to the others, all the dimensions are equivalent to parametrize the dune size. We choose the width w as it is directly involved in the expression of the sand flux at the rear of the dune. Figure 3 shows the inverse of the propagation velocity of the dune as a function of w. The velocity decreases as the inverse of the size:

$$\dot{x} \sim \frac{aQ}{w + w_c}. \tag{6}$$

The transverse velocity $\dot{y}$ is found to be null, as lateral inhomogeneities of the sand flux are unable to move dunes sideways [44]. The volume V of the dune is plotted on Fig. 4 as a function of its width. This relation is well fitted by

$$V = bw^2(w + w_v), \tag{7}$$

where the numerical coefficients are $b \sim 0.011$ and $w_v \sim 22.9$. This value roughly corresponds to the volume of a half pyramid, with a height $h \sim 0.1w$ and a width w which gives a volume $V \sim w^3/60$. One can observe that barchan dune are not self-similar object: the deviation observed for small dunes is related to the change of shape due to the existence of a characteristic length L. The field data obtained on eight dunes by Sauermann *et al.* [27] are consistent with Eq. (7) and with the value of L determined from the velocity/width relationship (Figs. 3 and 4).

C. Instabilities

The choice of the boundary conditions is absolutely crucial: to get stationary solutions, the sand escaping from the dune and reaching the downwind boundary is uniformly reinjected at the upwind one. Obviously, this ensures the overall mass conservation. Doing so, the simulation converges to a barchan of well defined shape of width w_∞ with a corresponding sand flux q_∞.

However, under natural conditions, the input flux q is imposed by the upwind dunes. We thus also performed simulations with a given and constant incoming flux. Figure 5 shows the evolution of two dunes of different sizes under an imposed constant input flux. One is a bit larger than the steady dune corresponding to the imposed flux, and the other is slightly smaller. It can be observed that none of these two initial conditions lead to a steady propagative dune: the small one shrinks and eventually disappears while the big one grows for ever. The steady solution obtained with the reinjection of the output flux is therefore unstable.

If solitary dunes are unstable, it is still possible that the interaction between dunes could stabilize the whole field. It is not what happened in the C_C^C model. Instead, an efficient coarsening takes place as shown by Sauermann in Chap. 8 of [41].

As a first conclusion, the C_C^C model predicts that solitary barchans and barchan fields are unstable in the case of a permanent wind. We will see below that these two instabili-
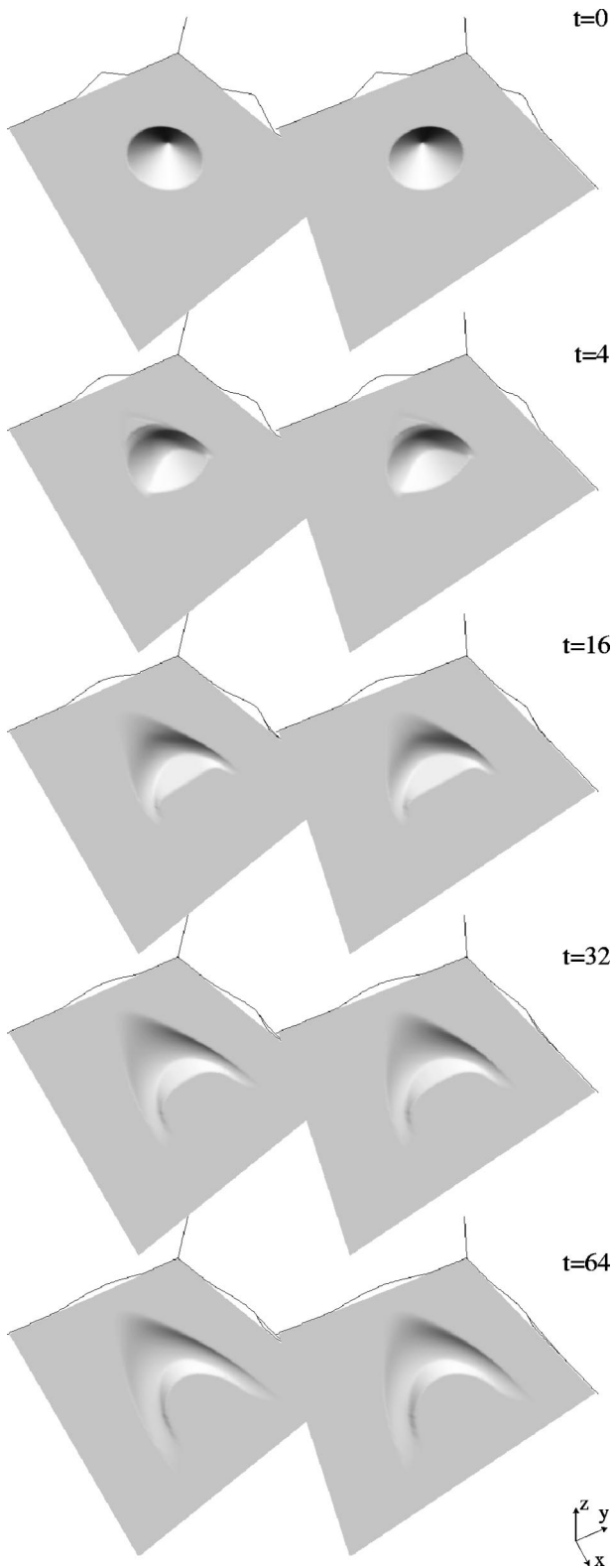
FIG. 2. Evolution from a conical sand pile to a steady propagative barchan of width 63 L computed from the C_C^C model. To obtain this steady solution the output flux is reinjected homogeneously at the upwind boundary. Times are given in units of L^2/Q. Stereoscopic view: (a) place the figure at ~60 cm from your eyes; (b) focus behind the sheet, at infinity (you should see three dunes); (c) focus on the middle dune and relax; (d) you should see the shape in 3D.
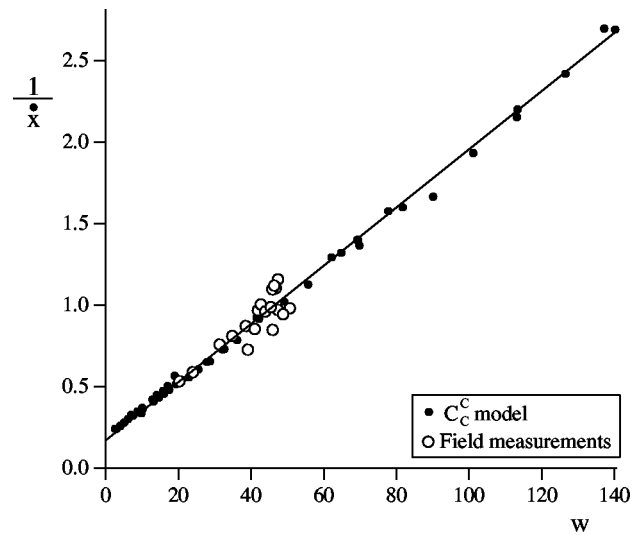

FIG. 3. Relationship between the inverse velocity $1/\dot{x}$ and the width w. Black dots: numerical simulations of barchans in the steady state. Open circles: field measurements on barchans from the region of Fig. 1 over a period of 27 yr rescaled by $Q = 66$ m^2/yr and $L = 3.5$ m. The line corresponds to the best fit by a Bagnold-like relation of the form $\dot{x} = aQ/(w + w_c)$. It gives $a = 56$ and $w_c = 9.5$.

ties are generic and not due to some particularity of the modeling. In particular, they can be also observed with the more complicated equations of Kroy, Sauermann, and Hermann who deal with a nonlinear charge equation and take explicitly into account the existence of a shear stress threshold to get erosion.
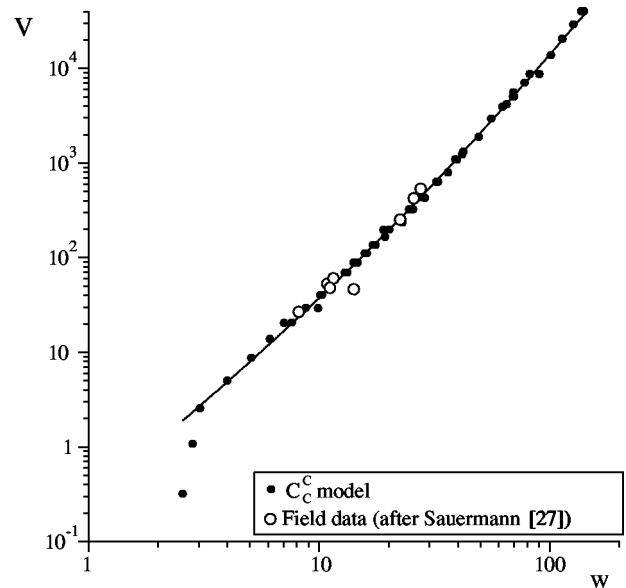

FIG. 4. Relationship between the volume V and the width w of barchans. Black dots: numerical simulations of solitary barchans in the steady state. White circles: field measurements on barchans from the region of Fig. 1 obtained by Sauermann *et al.* [27] rescaled by $L = 3.5$ m. Note the log-log scales. The solid line corresponds to the best fit by the relation $V = bw^2(w + w_v)$. It gives $b = 0.011$ and $w_v = 22.9$.
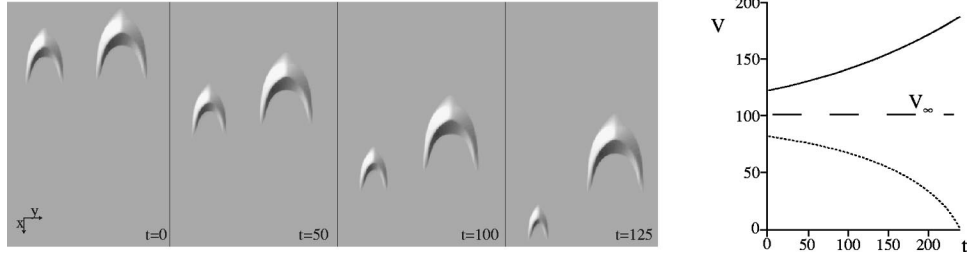
FIG. 5. Origin of the flux instability. Two dunes of initial widths 13.8 L and 16.6 L are submitted to a given flux, which is not the equilibrium sand flux for both dunes. The small dune (dotted line) is then under supplied an can only shrink. On the contrary, the bigger dune (solid line) receive too much sand and grows. The time evolution of their volume V, calculated from simulations of the C_C^C model, is shown on the right. Eventually, the small one disappears.

Therefore, we can wonder what the dynamical mechanisms responsible for these instabilities are. Would they have time/length to develop in an actual barchan field? Seeking answers to these questions, we will now investigate the two instabilities in a more general framework. As a first step, we will investigate the time and length scales associated to the evolution of barchan dunes.

II. TIME AND LENGTH SCALES

Three different time scales govern the dynamics of dunes: a very short one for aerodynamic processes (i.e., the grain transport), the turnover time for the dune motion, and a much larger time scale involved in the evolution of the dune volume and shape under small perturbations of the wind properties.

A. Turnover time

The dune memory time is usually defined as the time needed to propagate over its own length. Since the length and the width of the dune are almost equal—this is only a good approximation for steady dunes—we will use here the turnover time:

$$\tau_t = \frac{w}{\dot{x}}. \tag{8}$$

In the geological community, the turnover time is believed to be the time after which the dune looses the memory of its shape. The idea is that a grain remains static inside the dune during a cycle of typical time τ_t: it then reappears at the surface and is dragged by the wind to the other side of the dune. In other words, after τ_t all the grains composing a dune have moved, and the internal structure of the dune has been renewed. But this does not preclude memory of the dune *shape* at times larger than τ_t, and one can wonder whether τ_t is the internal relaxation time scale to reach its equilibrium shape. The scaling (6) of the propagation speed involves the cutoff length scale w_c, which can be measured by extrapolating the curve of Fig. 3 to zero. Note that the existence of a characteristic length scale also appears in the dune morphology [27,28,40,41]. In the following, we will assume that the barchans are sufficiently large to be considered in the asymptotic regime. We checked that introducing cutoffs w_c or w_v to capture the shape of curves like that of Figs. 3 or 4

in the region of small w does not change qualitatively the results. In the following we then take $w_c = 0$ and $w_v = 0$ for simplicity. Under this assumption, using the expression (6) of the propagation speed, the turnover time reads

$$\tau_t = \frac{w^2}{aQ}. \tag{9}$$

Of course, the length scale λ_t associated with the turnover time is the size of the dune itself:

$$\lambda_t = w. \tag{10}$$

B. Relaxation time

Let us consider, now, a single barchan dune submitted to a uniform sand flux. The evolution of its volume is governed by the balance of incoming ϕ_{in} and escaping ϕ_{out} sand volumes per unit time:

$$\dot{V} = \phi_{in} - \phi_{out}. \tag{11}$$

ϕ_{in} is directly related to the local flux q upwind the dune, defined as the volume of sand that crosses a horizontal unit length line along the transverse direction y per unit time. Assuming that this flux q is homogeneous, the dune receives an amount of sand simply proportional to its width w:

$$\phi_{in} = qw. \tag{12}$$

The loss of sand ϕ_{out} is not simply proportional to w because the output flux is not homogeneous. Figure 6 shows the flux in a cross section immediately behind the dune. One can see that the sand escapes only from the tip of the horns, where there is no more avalanche slip face. As a matter of fact, the recirculation induced behind the slip face traps all the sand blowing over the crest. We computed in the model the output flux ϕ_{out} as a function of the dune width w (Fig. 7). Within a good approximation it grows linearly with w:

$$\phi_{out} \sim Q(\Delta + \alpha w). \tag{13}$$

For the set of parameters chosen, the best fit gives $\alpha = 0.05$ and $\Delta = 1.33L$. Note that the discrepancy of ϕ_{out} with this linear variation for small dunes can be understood by the progressive disappearance of the slip face (domes), leading to a massive loss of sand.
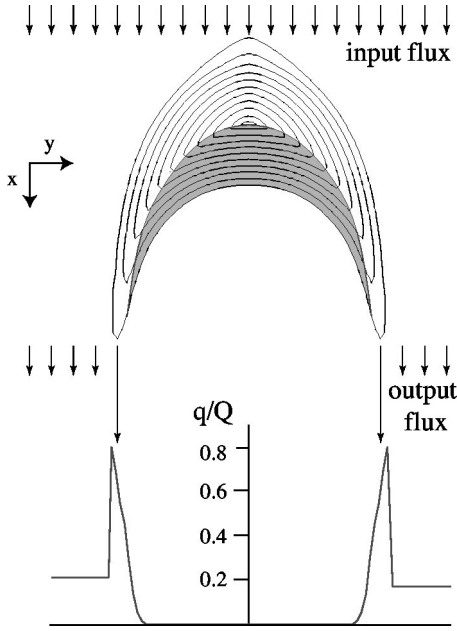
FIG. 6. Top: three dimensional shape of a barchan dune of width $33\,L$ obtained with the C_C^C model, with semiperiodic boundary conditions to ensure the mass conservation. Bottom: profile of the resulting output sand flux. The sand loss is localized at the tips of the horns. There, the flux is almost saturated: $q \sim Q$.

FIG. 7. Output flux ϕ_{out} as a function of the barchan width w for the equilibrium input flux (white circles) and for a null input flux (black circles). ϕ_{out} is not simply proportional to w and does not vanish at small size. As a consequence, the sand loss is proportionally smaller for a large dune than for a small one. The straight line corresponds to the best fit by a function of the form $\phi_{out} = Q(\Delta + \alpha w)$. It gives $\Delta = 1.33$ and $\alpha = 0.05$. Contrarily to velocity and size, no field measurements of the output flux have been conducted so far.

It can be observed from Fig. 6 that q is almost saturated in the horns. The ratio ϕ_{out}/Q then has a geometrical interpretation as it gives an estimate of the size of the horn tips. Therefore, in the C_C^C model, the horn size is not proportional to the dune width, but grows as $\Delta + \alpha w$. This is consistent with the observations made by Sauermann *et al.* in southern Morocco: they claim that, at least for symmetric solitary dunes, the slip face is proportionally larger for large dunes than for small ones, i.e. that the ratio of the horns width to the barchan width decreases with w.

With these two expressions for the input and output volume rates, the volume balance reads

$$\dot{V} = qw - Q(\alpha w + \Delta). \tag{14}$$

If we call w_∞ and q_∞ the width and the flux of the steady dune for which the dune volume is constant ($\dot{V} = 0$), we can define $\tau_r = (V - V_\infty)/\dot{V}$, taken around the fixed point. We get

$$\tau_r = \frac{3bw_\infty^3}{Q\Delta}. \tag{15}$$

It also gives us the relaxation length for the dune λ_r, which is the distance covered by the dune during the time τ_r, i.e.,

$$\lambda_r = \frac{3abw_\infty^2}{\Delta}. \tag{16}$$

C. Flux screening length

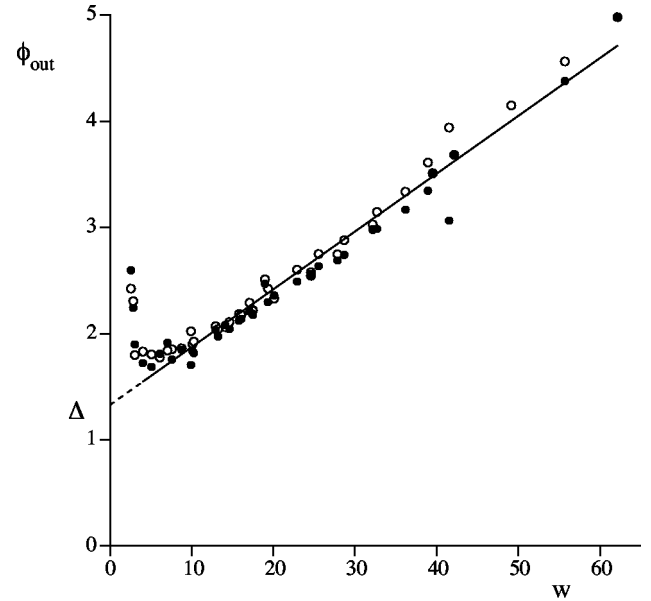For a dune field, the situation is a little bit more complex. The flux at the back of one dune is due to the output flux of an upwind dune. The latter is strongly inhomogeneous since the sand is only lost by the horns (Fig. 6). Field observations show that there is a sand less area downwind of the barchans—see also the inset of Fig. 8. This zone is larger than the recirculation bubble and indicates a small amount of sand trapped by the roughness of the ground. The fact that this ''shadow'' heals up is a signature of a lateral diffusion of the sand flux. The length of the shadow is typically a few times the dune width and is in general smaller than the distance between dunes. So, the flux can be considered as homogeneous when arriving at the back of the next dune.

The distance λ_q over which the flux changes is thus the distance, along the wind direction, between two dunes. It is the mean free path of one grain traveling in a straight line along the wind direction. Let us consider an homogeneous dune field composed of identical dunes of width w_∞. The number of dunes per unit surface is N_∞. It can be inferred from Fig. 8 that on average there is one dune in the surface $\lambda_q w_\infty$ (colored in gray on Fig. 8). The flux screening length thus depends on the density of dunes as

$$\lambda_q = \frac{1}{N_\infty w_\infty}. \tag{17}$$

Note that this length is larger than the average distance $(N_\infty)^{-1/2}$ between dunes—just like the mean free path in a gas. Since the grains in saltation on the solid ground go much faster than the dune (by more than five orders of magnitude), the flux screening time τ_q can be taken as null:
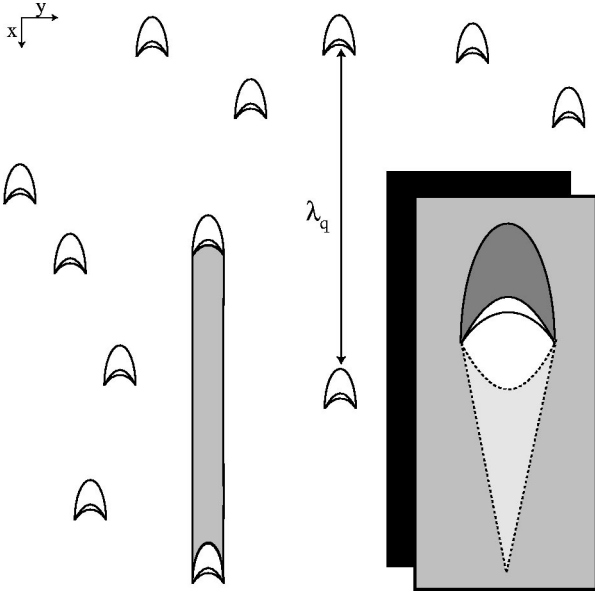
FIG. 8. The flux screening length is the mean free path along the wind direction. In other words, it is the mean longitudinal distance between two dunes. Inset: the sand flux is much larger on the back of the dune (dark zone) than on the surrounding ground (gray zone). Downwind the dune, it becomes inhomogeneous and in particular, it is null inside the recirculation bubble (white zone) and low in the triangular shadow zone (light gray). After a few dune sizes, the diffusion of grains rehomogenizes the flux.

$$\tau_q = 0. \tag{18}$$

D. Orders of magnitude

These different time scales can be estimated using the orders of magnitude obtained from field observations in the region of Fig. 1 coupled with the functional forms given by the C_C^C modeling. Fields measurements of the displacement of the dunes shown on Fig. 1 over 27 years have given $aQ = 3700$ m^2/year and $w_c = 33$ m. The C_C^C model relates w_c to L (Fig. 3) so that the saturation length can be estimated to $L \sim 3.5$ m. Similarly, the model gives 56 for the value of a which allows to deduce the estimate of $Q \sim 66$ m^2/year, which is compatible with direct measurements. These values give for the minimal horn width $\Delta \sim 4.6$ m.

Let us consider a small dune of width 20 m and a large dune of width 100 m belonging to the corridors of dunes shown on Fig. 1. The distance λ_r covered by the dune before the equilibrium between the size and the sand flux be reached is respectively 160 m and 4 km. In all the cases, it is much smaller than the dune field extension (typically 300 km corresponding to 15 000 small dune widths or 3000 large dune widths). Obviously, λ_r is much larger than the turnover length $\lambda_t = w$, and it is therefore clear that the turnover scales does not represent the memory of the dune.

The density of dunes can be inferred from Fig. 1 and is around $0.1/w_\infty^2$ (the average distance between dunes is around 3 dune sizes). Directly from Fig. 1 or from formula (17), the flux adaptation length λ_q is around 10 dune sizes, i.e., 200 m for the small dune and 1 km for the large one. Obviously, λ_q can be very different from place to place. For

instance, the left corridor shown on Fig. 1 is much denser than the third from the left. If the density of small dunes is $1/w_\infty^2$ instead of $0.1/w_\infty^2$, λ_q becomes equal to the dune size (20 m).

Using the previous value of Q, the dune velocities are 180 m/year and 37 m/year for the 20 m and 100 m barchans, respectively. The corresponding turnover times τ_t are 5.2 weeks and 2.7 years, while the relaxation time τ_r is as large as 10 months for the small dune and 1.1 centuries for the large one. Finally, the flux adaptation time τ_q is equal to the flux screening length λ_q divided by the grain speed (~ 1 m/s). It can thus be estimated to 3 minutes for the 20 m barchan and 16 minutes for the 100 m one.

The scale separation of the three times is impressive. $\tau_q \sim 3$ minutes $\ll \tau_t \sim 5.2$ weeks $\ll \tau_r \sim 10.4$ months for the small dunes, whereas for the large ones it reads $\tau_q \sim 16$ minutes $\ll \tau_t \sim 2.7$ years $\ll \tau_r \sim 1.1$ century. This shows that the annual meteorological fluctuations (wind, humidity) have potentially important effects: the actual memory time is always larger than seasonal time.

Sauermann has estimated a characteristic time for the evolution of the volume of a 100 m wide dune. He found several decades [41], which is comparable to the value we found for τ_r. On this basis he concluded that "considering this timescale it is justified to claim that barchans in a dune field are only marginally unstable." This is an erroneous conclusion as the length λ_r (4 km for $w = 100$ m) should be compared to the coherent corridors size (~ 50 km). Moreover, for small dunes as those on the left corridor of Fig. 1, λ_r is found to be as small as 160 m which is of the order of one hundredth of the portion of field displayed on the photograph. The evolution time and length scales could be thought as "very large"—with respect to human scales—but compared to the dune field size, they turn out to be small. Therefore, barchans have in fact the time and space to change their shape and volume along the corridors.

III. FLUX INSTABILITY

A. Stability of a solitary barchan

We seek to understand the generality of the instabilities revealed by the C_C^C model. We will first investigate theoretically the stability of a solitary dune in a constant sand flux q. We recall that the overall volume of sand received by this dune per unit time is simply proportional to its width: $\phi_{in} = qw$. As found in the C_C^C model, we suppose that $\phi_{out} = Q(\Delta + \alpha w)$ (Fig. 9 left). Let us investigate what happens for different values of the input flux q.

If $q < \alpha$ (dot-dashed line) the two curves $\phi_{in}(w)$ and $\phi_{out}(w)$ do not cross, which means that no steady solution can be found. Since the input sand volume rate is too low, any dune will shrink and eventually disappear. On the other hand, a fixed point w_∞ does exist for $q > \alpha$ (thin solid line). Suppose that this dune is now submitted to a slightly larger (respectively smaller) flux q (dotted lines): it will grow (respectively shrink). However, the corresponding steady states are respectively smaller and larger, so that they cannot be
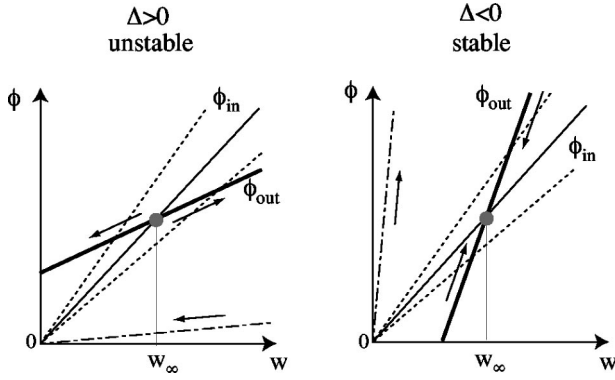
FIG. 9. The output volume rate $\phi_{out} = Q(\Delta + \alpha w)$ gives, when compared to the input rate $\phi_{in} = qw$, steady solutions that are unstable if $\Delta > 0$, and stable if $\Delta < 0$. The main point is to see whether the two lines cross from below or above at the steady point.

reached dynamically. We now fix the input flux to q_∞ and change the dune size w, as in Fig. 5. A dune of width slightly smaller than w_∞ will shrink more and more because it loses more sand than it earns. In a similar way, a dune larger than w_∞ will ever grow. In other words, the steady solutions are unstable.

This mechanism explains the flux instability of C_C^C barchans. This stability analysis is in fact robust and not specific to the linear choice for ϕ_{out}. Any more complicated function would lead to the same conclusion provided that ϕ_{in} crosses ϕ_{out} from below. The stability only depends on the behavior of the ϕ's in the neighborhood of the steady state.

How could a solitary barchan be stable? It is enough that ϕ_{in} crosses ϕ_{out} from above. Without loss of generality, we can keep a linear dependence of ϕ_{out} on w in the vicinity of the fixed point, but this time with $\Delta < 0$ (Fig. 9 right). In this case, the situation for which the input sand flux q is larger than α (dot-dashed line) leads to an ever growing dune. Steady solutions exist when $q < \alpha$. Because a smaller (resp. larger) sand flux now corresponds to a smaller (resp. larger) dune width, these solutions are, by contrast, stable.

In a more quantitative and formal way, the mass balance for a barchan (14) can be rewritten in terms of the dune width only:

$$\dot{w} = \frac{q_\infty w - Q(\Delta + \alpha w)}{3bw^2}. \tag{19}$$

Linearizing this equation around the fixed point w_∞ we obtain

$$\tau_r \dot{w} = w - w_\infty. \tag{20}$$

The sign of the relaxation time τ_r is that of Δ—see relation (15). Therefore if Δ is positive, w will quickly depart from its steady value w_∞. In the inverse case $\Delta < 0$, any deviation of w will be brought back to w_∞.

In summary, the stability of a solitary barchan depends on whether the ratio of the output volume rate to its width ϕ_{out}/w increases or decreases with w. This quantity is perhaps not easy to measure on the field but we have shown that

it is directly related to the ratio of the size of the horn tips to the dune width. If viewed from the face, the horn tips become in proportion smaller as the dune size increases, the barchan is unstable. This is what is predicted by the C_C^C model, in agreement with the few field observations [27]. (See Figs. 10 and 11.)
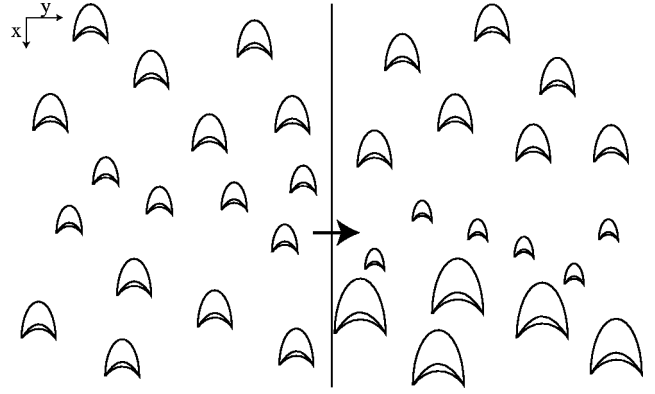

FIG. 10. Sketch showing the instability due to the exchange of mass between the dunes: dunes slightly smaller than w_∞ lose sand and make their downwind neighbors grow. Note that the dune field is assumed to remain locally homogenous.

B. Stability of a dune field

At this point, the stability analysis leads to the fact that a single solitary barchan is unstable. Could then dunes be stabilized by their interaction via the sand flux? Let us consider a dune field which is locally homogeneous and composed, around the position (x, y), barchans of width w with a density N. We ignore for the moment the fact that dunes can collide. The conservation of the number of dunes then reads

$$\dot{N} = \partial_t N + \partial_x(\dot{x}N) + \partial_y(\dot{y}N) = 0. \tag{21}$$

The Eulerian evolution of the dunes width is given by

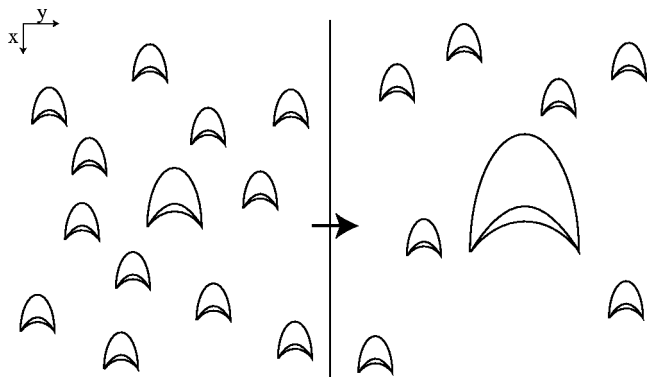$$\dot{w} = \partial_t w + \dot{x}\partial_x w + \dot{y}\partial_y w. \tag{22}$$

FIG. 11. Sketch showing the instability due to the collisions between the dunes. If one dune is slightly larger than the others, it goes slower and will absorb incoming dunes.

This equation has to be complemented by the equation governing the evolution of the sand flux q between the dunes which results from the variation of the volume of these dunes (and reciprocally):

$$\partial_x q = -N\dot{V}. \tag{23}$$

These three equations can be closed using the previous modeling of $\dot{x}$, $\dot{y}=0$, $\dot{w}$ and $\dot{V}=3bw^2\dot{w}$. Any homogeneous field of barchans of width w_∞ and density N_∞ is a solution, provided that there is a free flux $q_\infty = Q(\Delta/w_\infty + \alpha)$ between the dunes.

We are now interested in the stability of this solution towards locally homogeneous disturbances. Note that such a choice is still consistent with equations that do not take collisions into account. We thus expand w, q and N around their stationary values w_∞, q_∞, N_∞, and introduce the length and time scales λ_r, λ_q and τ_r. We get

$$\tau_r\partial_t N + \lambda_r\partial_x N - \frac{N_\infty}{w_\infty}\lambda_r\partial_x w = 0, \tag{24}$$

$$\tau_r\partial_t w + \lambda_r\partial_x w = (w-w_\infty) + \frac{w_\infty^2}{Q\Delta}(q-q_\infty), \tag{25}$$

$$\lambda_q\partial_x q = -(q-q_\infty) - \frac{Q\Delta}{w_\infty^2}(w-w_\infty). \tag{26}$$

Without loss of generality we can write the disturbances under the forms: $q-q_\infty = q_1 e^{\sigma t+ikx}$, $w-w_\infty = w_1 e^{\sigma t+ikx}$ and $N-N_\infty = N_1 e^{\sigma t+ikx}$. Solving the system of linear equations we obtain the expression of the growth rate σ as a function of the wave number k:

$$\tau_r\sigma = ik\left(\frac{\lambda_q}{1+(k\lambda_q)^2} - \lambda_r\right) + \frac{(k\lambda_q)^2}{1+(k\lambda_q)^2}. \tag{27}$$

The sign of the real part of the growth rate σ is that of τ_r and thus of Δ. The stability of the dune field is therefore that of the solitary dune. If $\Delta < 0$, which means that all the individual dunes are stable, the field is (for obvious reasons) stable. But in fact, all the individual dunes are unstable ($\Delta > 0$), so that a field in which dunes interact via the sand flux is also unstable.

The result of the above formal demonstration can also be understood via a simple argument illustrated on Fig. 10. Consider a barchan dune field at equilibrium: for each dune, input and output volume rate are equal. Now, imagine that the input flux of a dune slightly decreases for some reasons. As explained in the previous subsection, if this dune is unstable ($\Delta > 0$) it tends to shrink. Consequently its output flux increases, and makes its downwind neighbors grow. Therefore, even a small perturbation of the sand flux can dramatically change the structure of the field downwind.

IV. COLLISIONAL INSTABILITY

The free flux is not the only way barchans can influence one another. If sufficiently close, they can interact through the wind, i.e., aerodynamically. This is possible when the dunes get close to each other. In this case, they actually collide. We therefore would like to investigate the behavior of one particular dune in the middle of the field.

Let us consider a homogeneous field of barchans of width w_∞, with an additional dune of size $w=(1+\eta)w_\infty$. The variation of the volume of this dune is due to the sand flux as well as the collisions of incoming dunes. These collisions are a direct consequence of the fact that smaller dunes travel faster [Eq. (6)]. The number of collisions per unit time is proportional to the dune density N_∞ times the collisional cross section $w+w_\infty$ times the relative velocity $aQ(1/w_\infty - 1/w)$. We assume that the collisions lead to a merging of the two dunes. Then, each collision leads to an increase of the mass of the larger dune by $V_\infty = bw_\infty^3$. We can then write for this particular dune:

$$\dot{V} = qw - Q(\alpha w + \Delta) + N_\infty V_\infty(w+w_\infty)\frac{aQ(w-w_\infty)}{ww_\infty}. \tag{28}$$

Introducing a critical dune density N_c as

$$N_c = \frac{-\Delta}{2abw_\infty^3}, \tag{29}$$

the equation governing the evolution of the width of the dune considered reads

$$\tau_r\dot{\eta} = \left(1 - \frac{(2+\eta)}{2(1+\eta)}\frac{N_\infty}{N_c}\right)\frac{\eta}{(1+\eta)^2}. \tag{30}$$

Note that, rigorously speaking, N_c is a positive quantity and thus a true density only for $\Delta < 0$ (see below). Figure 12 shows $\dot{\eta}$ as a function of the dune size. Expanding linearly around $\eta = 0$, we obtain the growth rate $\sigma = \dot{\eta}/\eta$ as

$$\tau_r\sigma = 1 - \frac{N_\infty}{N_c}. \tag{31}$$

Therefore, if the dunes are individually unstable [case $\Delta > 0$, Fig. 12(a)], the dunes are always unstable towards the collisional instability. The barchan field quickly merge into one big barchan dune. If the dune are individually stable ($\Delta < 0$), the same instability develops but only when the dune density is larger than the critical dune density N_c [Fig. 12(b)]. Suppose indeed that one collision occurs in the middle of an homogeneous field, creating a dune of twice its original volume. Since it is larger, this dune slows down and a second collision occurs before the large dune has recovered its equilibrium. If now the dune density is small [Fig. 12(c)], the time before a second collision happens is sufficiently large to allow the large dune to recover its equilibrium volume, and in this case a field of stable dunes is stable towards the collision process.

V. BARCHANS CORRIDORS, AN OPEN PROBLEM

The aim of this conclusion is twofold. We will first give a summary of the different results presented in this paper. Then
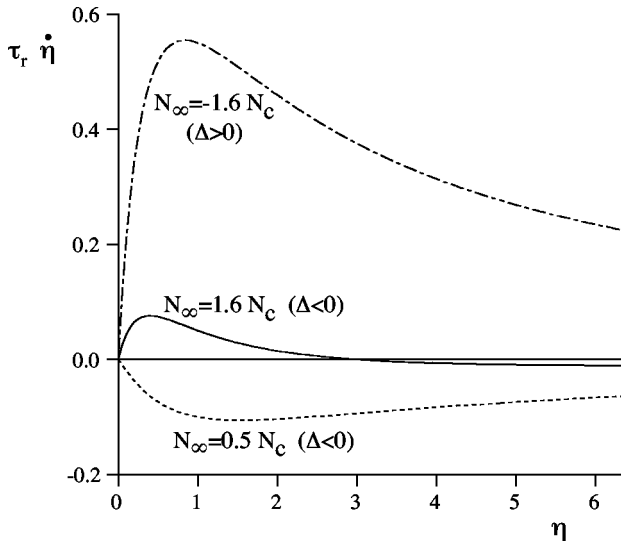
FIG. 12. Growth rate $\tau_r \dot{\eta}$ of a dune due to collisions, as a function of the rescaled size η in three different cases. If the solitary dune is unstable ($\Delta > 0$), the field is also unstable towards the collisional instability (dot-dashed line). If the solitary dune is stable ($\Delta < 0$), the stability of the field depends on the dune density. At high density (solid line), the field is linearly unstable while at low density (dashed line), it is stable towards any disturbance.

we will discuss the problem of the size selection and the formation of barchans corridors.

The starting point of the present work is the observation that barchan dunes are organized in fields stretched along the dominant wind direction (Fig. 1) that can be as long as 300 km. These barchans corridors are quite homogeneous in size and in spacing. For instance, the barchans field between Tarfaya and Laayoune presents a zone of 50 km without any geological obstacle in which the same five coherent corridors persist. This size selection is of course not to be taken in a strict sense: there are large fluctuations from one dune to another, which have *also* to be explained.

We have shown that the stability of a solitary dune essentially depends on the relationship between the size of the horns and that of the dune. Indeed, the dune receives at its back a sand flux proportional to its size but releases sand only by its horns. If the size of the horns is proportionally smaller for large dunes than for small ones, the steady state of the dune is unstable: it either grows or decay (Fig. 10). If, on the contrary, the sand leak increases faster than the dune size, it pulls the dune back to equilibrium. Furthermore we have shown that the fact that a dune is fed by the output flux of the dunes upwind does not change the stability analysis. This is essentially because a dune can influence another dune downwind through the flux but there is no feedback mechanism.

We are thus left with a secondary question: how does the horns width evolve with the dune size? The only field measurements from which the horns size can be extracted are the shape measurements of eight dunes by Sauermann *et al.* [27]. The sum of the width of the two horns is found to be between 12 and 28 m for the five small dunes they measured

(2 and 3 m high), and between 12 and 17 m for the three larger ones (heights between 6 and 8 m). If we trust the relevance of their selection of dunes, this means that the horn size is almost independent of that of the dune. This is also coherent with their claim that the slip face is proportionally smaller and the horns larger for small dunes than for large ones. In that case, solitary barchans should be individually unstable.

The second indication is provided by the C_C^C modeling, with which we recover that this steady state is in fact unstable (Figs. 5 and 7), in fact for the very same reasons as above. The solution can be artificially stabilized by putting at the back of the dune exactly what it loses by its horns but this is only a numerical trick. What determines the size of the horns in the model? The 3D solutions can be thought of coupled 2D solutions [28]. Then, the horns start when there is no slip face, i.e., when the length becomes of the order of the minimal size of dunes. This simple argument leads to think that the horns should keep a characteristic size of order of few saturation lengths L whatever the dune size is.

We have shown that there is a second robust mechanism of instability. We know from field measurements, numerical models and theoretical analysis that the dune velocity is a decreasing function of its size. The reason is simply that the flux at the crest is almost independent of the dune size and will make a small dune propagate faster than a large one. This is sufficient to predict the coarsening of a dune field: because they go faster, small dunes tend to collide the large ones making them larger and slower. This collision instability should also lead to an ever growing big dune.

The scales over which all instabilities develop are the relaxation time τ_r and length λ_r. For the eastern corridor of Fig. 1, the order of magnitude of the dune width is 100 m which gives $\tau_r \sim 1.1$ century and $\lambda_r \sim 4$ km. For the western corridors, the dunes are smaller ($w \sim 20$ m and the characteristic scales become $\tau_r \sim 10$ months and $\lambda_r \sim 160$ m. These lengths are much smaller than the extension of the corridor (300 km) so that these instabilities have sufficient space to develop.

However, the actual barchan corridors are homogenous and one cannot see any evidence of such instabilities. As a conclusion, the dune size selection and the formation of barchan corridors are still open problems in the present state of the art. There should exist another robust dynamical mechanism leading to an extra leak of the dunes, to balance the collisional and the flux instabilities. There are already two serious candidates for this mechanism. First, we do not have any information on the collision process, which could lead in reality to the formation of several dunes. Second, we have only investigated here the case of a permanent wind. We have shown that the dunes characteristic times are larger than one year so that the annual variations of the wind regime could have drastic effects. Figure 13 shows aerial photographs of eight barchan dunes. They all present a periodic array of 1 m high slip faces on their left side reminiscent of a secondary wind (probably a storm) coming from the west (from the left on the figure). This new instability related to changes in wind direction could lead to a larger time averaged output flux than expected for a permanent wind. Further
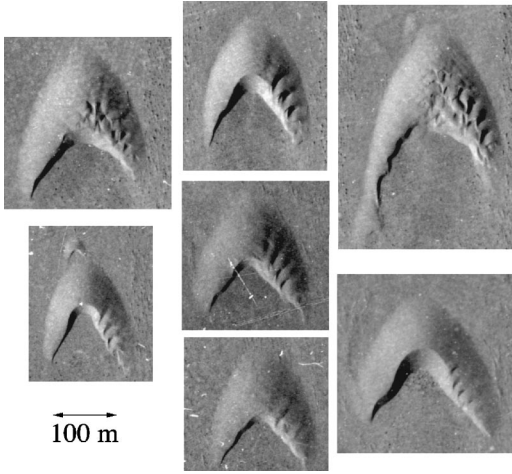
FIG. 13. Aerial photographs of several barchan dunes in the same region as the field of Fig. 1. They all exhibit an instability on the left side, leading to a periodic array of small slip faces.

work in that direction will perhaps shed light on the formation of nearly homogeneous corridors of barchan dunes.

ACKNOWLEDGMENTS

APPENDIX: THE 3D C_C^C MODEL

The three starting equations of the model are the conservation of matter, the charge equation and the coupling between the saturated flux and the dune shape h:

$$\partial_t h + \partial_x q = D \vec{\nabla} \cdot (q \vec{\nabla} h), \tag{A1}$$

$$\partial_x q = \frac{q_{sat} - q}{L}, \tag{A2}$$

$$\frac{q_{sat}}{Q} = 1 + A \int \frac{d\chi}{\pi(\chi - x)} \partial_x h_e + B \partial_x h_e. \tag{A3}$$

We recall that the overall flux is the sum of q along the wind direction, plus an extra flux due to reptons along the steepest slope. The two last equations do not contain any y dependence and can thus be solved for each slice in x independently, using a discrete scheme in space of mesh size dx. The conservation of matter (A1) couples the slices through the diffusion term and is solved by a semi-implicit scheme of time step dt. To speed up the numerical computation of the saturated flux, we use the discrete Fourier transform $\mathcal{F}$ of the dune envelope h_e:

$$q_{sat} = Q[1 + \mathcal{F}^{-1}(\mathcal{F}(h_e)(A|k| + iBk))]. \tag{A4}$$

This envelope is composed of the dune profile $h(x)$ up to the point where the turbulent boundary layer separates:

TABLE I. Parameters used for the C_C^C computation.

$A = 4.7$	curvature effect
$B = 5.0$	slope effect
$D = 0.1$	Lateral diffusion
$\mu_b = 0.25$	separation slope
$E = 50$	avalanches
$\mu_d = 0.5$	avalanche slope
$dx = 0.25 - 1.0$	mesh size
$dt = 0.001 - 0.1$	time step
$M = 64 - 512$	box size

$$x < x_b : h_e(x) = h(x). \tag{A5}$$

In the absence of any systematic and precise studies on this separation bubble, we assume that the separation occurs when the slope is locally steeper than a critical value $\mu_b = 0.25$:

$$h(x_b) - h(x_b + dx) > \mu_b dx. \tag{A6}$$

When the dune presents a slip face, the boundary layer thus separates at the crest. The separation streamline is modeled as a third order polynomial:

$$x_b < x < x_r : h_e(x) = a + bx + cx^2 + dx^3. \tag{A7}$$

The four coefficients are determined by smooth matching conditions:

$$h_e(x_b) = h(x_b), \quad h_e(x_b - dx) = h(x_b - dx), \tag{A8}$$

$$h_e(x_r) = h(x_r), \quad h_e(x_r + dx) = h(x_r + dx), \tag{A9}$$

and the reattachment point x_r is the first mesh point for which the slope is nowhere steeper than μ_b. There is no grain motion inside the recirculation bubble, so that the charge equation should be modified to $\partial_x q = -q$ for $x_b < x < x_r$. Similarly, on the solid ground ($h = 0$) no erosion takes place, so that $\partial_x q = 0$.

The last important mechanism is the relaxation of slopes steeper than μ_d by avalanching. Rather than a complete and precise description of avalanches of grains, we treat them as an extra flux along the steepest slope,

$$\partial_t h + \partial_x q = \vec{\nabla} \cdot [(Dq + E\delta\mu)\vec{\nabla}h], \tag{A10}$$

where $\delta\mu$ is nul when the slope is lower than μ_d and equal to $\delta\mu = |\vec{\nabla}h|^2 - \mu_d^2$ otherwise. For a sufficiently large coefficient E, the result of this trick is to relax the slope to μ_d, independently of E. Note that, as the diffusion of reptons, these avalanches couple the different 2D slices. The value of the parameters have been chosen to reproduce the morphological aspect ratios and are given in Table I. The results presented in this paper have been obtained for different discretization time and space steps, different box sizes and different total times.

[1] R. A. Bagnold, *The Physics of Blown Sand and Desert Dunes* (Chapman and Hall, London, 1941).

[2] P. R. Owen, J. Fluid Mech. **20**, 225 (1964).

[3] A. D. Howard, Bull. Geol. Soc. Am. **88**, 853 (1977).

[4] M. Sørensen, in *International Workshop on the Physics of Blown Sand*, edited by Barndorff-Nielsen, Moller, Rasmussen, and Willets (University of Aarhus, Aarhus, 1985), pp. 141–190.

[5] J. L. Jensen and M. Sorensen, Sedimentology **33**, 547 (1986).

[6] R. S. Anderson and P. K. Haff, Science **241**, 820 (1988).

[7] R. S. Anderson and P. K. Haff, Acta Mech. (Suppl) **1**, 21 (1991).

[8] R. S. Anderson, M. Sørensen, and B. B. Willetts, Acta Mech. (Suppl) **1**, 1 (1991).

[9] M. Sørensen, Acta Mech. (Suppl) **1**, 67 (1991).

[10] B. B. Willetts, J. K. McEwan, and M. A. Rice, Acta Mech. (Suppl) **1**, 123 (1991).

[11] K. R. Rasmussen and H. E. Mikkelsen, Acta Mech. (Suppl) **1**, 135 (1991).

[12] P. Nalpanis, J. C. R. Hunt, and C. F. Barrett, J. Fluid Mech. **251**, 661 (1993).

[13] J. D. Iversen and K. R. Rasmussen, Sedimentology **41**, 721 (1994).

[14] K. R. Rasmussen, J. D. Iversen, and P. Rautaheimo, Geomorphology **17**, 19 (1996).

[15] F. Rioual, A. Valance, and D. Bideau, Phys. Rev. E **62**, 2450 (2000).

[16] G. Sauermann, K. Kroy, and H. J. Herrmann, Phys. Rev. E **64**, 031305 (2001).

[17] B. Andreotti, J. Fluid Mech. (to be published).

[18] H. J. L. Beadnell, Geographical J. **35**, 379 (1910).

[19] H. J. Finkel, J. Geol. **67**, 614 (1959).

[20] A. Coursin, Bull. de l'IFAN **3**, 989 (1964).

[21] J. T. Long and R. P. Sharp, Geol. Soc. Am. Bull. **75**, 149 (1964).

[22] S. L. Hastenrath, Z. Geomorphologie **11**, 300 (1967).

[23] R. M. Norris, J. Geol. **74**, 292 (1966).

[24] S. L. Hastenrath, Z. Geomorphologie **31-2**, 167 (1987).

[25] M. C. Slattery, South African Geographical J. **72**, 5 (1990).

[26] P. A. Hesp and K. Hastings, Geomorphology **22**, 193 (1998).

[27] G. Sauermann, P. Rognon, A. Poliakov, and H. J. Herrmann, Geomorphology **36**, 47 (2000).

[28] B. Andreotti, P. Claudin, and S. Douady, Eur. Phys. J. B **28**, 341 (2002).

[29] P. Hersen, S. Douady, and B. Andreotti, Phys. Rev. Lett. **89**, 264301 (2002).

[30] K. R. Mulligan, Earth Surf. Processes Landforms **13**, 573 (1988).

[31] O. Zeman and N-O. Jensen, Q. J. R. Meteorol. Soc. **113**, 55 (1987).

[32] P. S. Jackson and J. C. R. Hunt, Q. J. R. Meteorol. Soc. **101**, 929 (1975).

[33] A. D. Howard, J. B. Morton, M. Gad el Hak, and D. B. Pierce, Sedimentology **25**, 307 (1978).

[34] N-O. Jensen and O. Zeman, in *International Workshop on the Physics of Blown Sand*, edited by Barndorff-Nielsen, Moller, Rasmussen, and Willets (Ref. [4]), pp. 351–368.

[35] F. K. Wippermann and G. Gross, Boundary-Layer Meteorol. **36**, 319 (1986).

[36] J. C. R. Hunt, S. Leibovitch, and K. J. Richards, Q. J. R. Meteorol. Soc. **114**, 1435 (1988).

[37] W. S. Weng, J. C. R. Hunt, D. J. Carruthers, A. Warren, G. F. S. Wiggs, I. Livingstone, and I. Castro, Acta Mech. (Suppl) **2**, 1 (1991).

[38] B. T. Werner, Geology **23**, 1107 (1995).

[39] J. H. van Boxel, S. M. Arens, and P. M. van Dijk, Earth Surf. Processes Landforms **24**, 255 (1999).

[40] K. Kroy, G. Sauermann, and H. J. Herrmann, Phys. Rev. Lett. **88**, 054301 (2002).

[41] G. Sauermann, Ph.D. thesis, Stuttgart University, edited by Logos Verlag, Berlin, 2001.

[42] B. Andreotti, P. Claudin, and S. Douady, Eur. Phys. J. B **28**, 321 (2002).

[43] K. Lettau and H. H. Lettau, Z. Geomorphologie **13**, 182 (1969).

[44] A. R. Lima, G. Sauermann, H. J. Herrmann, and K. Kroy, Physica A **310**, 487 (2002).

[45] P. Hersen, Eur. Phys. J. B (to be published).

[46] The success story of the barchan perhaps originates from the fact that cars can easily come close to their feet.